Dryland ecosystems: The coupled stochastic dynamics of soil water and vegetation and the role of rainfall seasonality

R. Vezzoli,[1,*] C. De Michele,[1,†] H. Pavlopoulos,[2,‡] and R. J. Scholes[3,§]
[1]*DIIAR, Politecnico di Milano, Milan, Italy*
[2]*Department of Statistics, Athens University of Economics and Business, Athens, Greece*
[3]*CSIR, Pretoria, South Africa*
(Received 15 November 2007; published 13 May 2008)

In drylands the soil water availability is a key factor ruling the architecture of the ecosystem. The soil water reflects the exchanges of water among soil, vegetation, and atmosphere. Here, a dryland ecosystem is investigated through the analysis of the local interactions between soil water and vegetation forced by rainfall having seasonal and stochastic occurrence. The evolution of dryland ecosystems is represented by a system of two differential equations, having two steady states, one vegetated and the other unvegetated. The rainfall forcing is described by a diffusion process with monthly parameters. In each of the two possible steady states, the probability density functions of soil water and vegetation are derived analytically in terms of the rainfall distribution. The results show how the seasonality of rainfall influences the oscillation of the ecosystem between its vegetated steady state during the wet season and its unvegetated steady state during the dry season.

DOI: 10.1103/PhysRevE.77.051908 PACS number(s): 87.23.Cc, 02.50.Ey, 92.60.Jq, 91.62.+g

I. INTRODUCTION

Drylands are environments where the existence and growth of vegetation depends principally on the availability of water in the soil. In this sense, drylands constitute water-limited ecosystems, whose evolution is governed by the dynamics of soil water and vegetation. These dynamics are strictly interrelated, since the vegetation takes up water from the soil for its transpiration, while concurrently it reduces water evaporation through its shadowing effect. Rainfall is the external force exciting and driving the coupled dynamics of soil water and vegetation. In the pertinent literature, the approach adopted toward modeling of the coupled dynamics of soil water and vegetation is usually deterministic, representing rainfall forcing as a constant parameter throughout time, e.g., see [1–4]. However, rainfall is notoriously variable, a fact suggesting that stochastic modeling is by far more appropriate. Some studies have investigated the dynamics of soil water content driven by a simple model of stochastic rainfall, according to which the entire volume of rainfall is concentrated on a discrete set of individual time instants as a marked point process, e.g., see [5,6]. The authors of [7] considered the dynamics of vegetation forced by a simple stochastic rainfall. Recently, the importance of driving the soil-water vegetation interactions by suitable stochastic processes modeling rainfall has been addressed numerically in [8–10] and analytically in [11]. In drylands, however, the rainfall has also a strong seasonal component. That is, the greatest portion of the annual amount of precipitation is concentrated in a certain period of the year, usually referred to as the *wet* (or rainy) *season*, while the rest of the year is referred to as the *dry season*, in the sense that precipitation becomes a rare event then. For example, in two-thirds of Africa the annual rainfall is distributed in approximately three months only, with high variability from one month to the other; see [12]. The authors of [4] have recognized the significance of rainfall seasonality, addressing its impact on the self-organization and productivity in semiarid ecosystems. In the present paper, we study the coupled dynamics of soil water and vegetation locally (i.e., at a single point of space), under the forcing of stochastic rainfall, accounting for both stochastic and seasonal occurrences and variability. Section II describes the interactions between soil water and vegetation in drylands. Section III furnishes a stochastic diffusion model for rainfall, with seasonally adjustable coefficients of drift and dispersion. Section IV illustrates the coupled stochastic dynamics of soil water and vegetation, providing analytical formulas for steady state probability distributions of both dynamic variables. Section V focuses on the impact of rainfall seasonality upon the coupled dynamics of soil water and vegetation, with particular reference to the steady states of the system.

II. SOIL-WATER VEGETATION INTERACTIONS

The soil-water–vegetation local interactions are described by the following pair of ordinary differential equations, proposed in [11]:

$$\frac{dS}{dt} = \frac{P}{w_1}(1-S) - \epsilon S(1-N) - \tau SN,$$

$$\frac{dN}{dt} = \gamma SN(1-N) - \mu N, \tag{1}$$

where P denotes the *rainfall rate*, i.e., the volume of precipitated water per time per area, S the *soil water* specified by

*renata.vezzoli@polimi.it
†carlo.demichele@polimi.it
‡hgp@aueb.gr
§bscholes@csir.co.za

the degree of saturation of the profile of available water capacity minus the residual soil water governed by capillary forces, and N the *normalized vegetation density* specified by the ratio between the aboveground vegetation density and the maximum value attainable (carrying capacity) in a given environment. The variables S and N are both dimensionless, taking values in the closed interval $[0,1]$, while $P \in [0,+\infty)$ carries dimension m/yr. The following conventions are meant to accompany Eqs. (1): (1) the ecosystem is water limited, in the sense that soil water availability is the only limiting factor; (2) the groundwater table is deep enough, so that it does not affect the soil water in the root zone, and itself is inaccessible to roots; (3) the model describes the soil water dynamics inside the root zone.

The first of Eqs. (1) describes the dynamics of S, where w_1 is the fraction of the pore volume available for water storage, with respect to a volume of unitary base and height equal to the root zone depth (m^3/m^2). ϵ and τ denote the evaporation and transpiration rates, respectively, each carrying dimension yr^{-1}. The term $\frac{P}{w_1}$ represents the rainfall rate normalized with respect to the root zone capacity. We assume that the soil surface is practically horizontal, and the entire quantity of rainfall infiltrates into the soil as long as the root zone capacity is not saturated. The term $\frac{P}{w_1}S$ models *percolation* beyond the root zone. When $S=0$ (completely dry soil) all the rainfall contributes to moistening of the root zone. When $S=1$ (saturated root zone) the rainfall percolates through the soil and is lost to the roots. The term $\epsilon S(1-N)$ models *evaporation* from the soil, proportional to S and reduced by the shading and boundary layer resistance effects of the vegetation, according to $(1-N)$. The term τSN models vegetation *transpiration* as being proportional to both S and N.

The second of Eqs. (1) represents the dynamics of N, where γ and μ denote rates of vegetation growth and depletion, respectively, each of dimension yr^{-1}. Vegetation dynamics is modeled by a logistic *growth* term $\gamma SN(1-N)$ and a term μN for vegetation *depletion*, proportional to N. Hereafter, we assume that w_1, ϵ, τ, γ, and μ remain constant; see [11]. Equations (1) capture the first-order (i.e., the most fundamental) features of the hydrological and ecological processes and their interactions, at a point, in drylands.

Soil moisture and vegetation have different time responses to rainfall forcing. From the first of Eqs. (1) it is seen that S is directly influenced by P, implying a faster response than N to P dynamics. From the second of Eqs. (1), it is seen that N is only indirectly influenced by P, through the dynamics of S. Thus, a *hysteresis effect* between the responses of S and N to P dynamics is anticipated. This effect is quantified by the time lag between the responses of N and S to a certain forcing P, denoted by τ_{S-N}. This time lag depends on the initial state of the system, and is indicative of the survival capacity of vegetation during dry periods, i.e., in absence of rainfall. Note that, when rainfall stops, i.e., $P=0$, immediately the derivative of S becomes negative, while the derivative of N becomes negative only when the condition $1-N<\mu/(\gamma S)$ is satisfied. As a random variable τ_{S-N} can be characterized through its mean $\mathbb{E}(\tau_{S-N})$ and standard deviation $\sigma(\tau_{S-N})$. We have calculated numerically these two quantities using 10 000 initial conditions, assuming $P(t)=0$, and considering two sets of parameters: one for grass vegetation ($w_1=0.35$ m, $\epsilon=4$ yr^{-1}, $\tau=5$ yr^{-1}, $\gamma=2$ yr^{-1}, and $\mu=0.4$ yr^{-1}), and one for tree vegetation ($w_1=0.35$ m, $\epsilon=4$ yr^{-1}, $\tau=4$ yr^{-1}, $\gamma=1$ yr^{-1}, and $\mu=0.1$ yr^{-1}). We obtain $\hat{\mathbb{E}}(\tau_{S-N})=26$ days ≈ 1 month and $\hat{\sigma}(\tau_{S-N})=34$ days ≈ 1 month for grass, and $\hat{\mathbb{E}}(\tau_{S-N})=55$ days ≈ 2 months and $\hat{\sigma}(\tau_{S-N})=56$ days ≈ 2 months for tree. These values are in agreement with those given in Table I of [13].

The system of Eqs. (1) admits two steady states ($\frac{dS}{dt}=\frac{dN}{dt}=0$), one unvegetated (or bare soil) state

$$S = \frac{1}{1+\frac{\epsilon}{P/w_1}}, \qquad N = 0, \tag{2}$$

and one vegetated state

$$S = \frac{1-\frac{\mu}{\gamma}\frac{\epsilon-\tau}{P/w_1}}{1+\frac{\tau}{P/w_1}}, \qquad N = \frac{1-\frac{\mu}{\gamma}\left(1+\frac{\epsilon}{P/w_1}\right)}{1-\frac{\mu}{\gamma}\frac{\epsilon-\tau}{P/w_1}}. \tag{3}$$

Equations (2) give acceptable physical states for any value of $P \geq 0$, while Eqs. (3) do so only for $P > \frac{\epsilon\mu w_1}{\gamma-\mu}$. The condition $P > \frac{\epsilon\mu w_1}{\gamma-\mu}$ is necessary to guarantee $N>0$, when $\gamma>\mu$. The local stability analysis shows that the bare soil solution remains stable as long as $P < \frac{\epsilon\mu w_1}{\gamma-\mu}$, while for values of P greater than this threshold the bare soil solution behaves locally as a saddle point. At the other end, the vegetated solution is locally stable for $P > \frac{\epsilon\mu w_1}{\gamma-\mu}$, or equivalently for $S > \frac{\mu}{\gamma}$.

In the vegetated solution, when $\gamma>\mu$ (as required for the onset of vegetation), it is easily seen that both S and N are (strictly) increasing smooth functions of P. The same is true for S, unconditionally, in the bare soil solution. The smoothness of S and N (i.e., existence of continuous derivatives up to second order), with respect to P in Eqs. (2) and (3), is instrumental in obtaining the steady state probability distributions of the temporal stochastic processes $\{S(t)\}$ and $\{N(t)\}$ from the stationary distribution of the stochastic precipitation process $\{P(t)\}$, in the framework of stochastic calculus. Indeed, given an appropriate diffusion model for the stochastic process $\{P(t)\}$, via Itô's formulas (e.g., see [14]) one may obtain (at least in principle) explicitly the stationary distribution of any smooth transformation of $\{P(t)\}$. In the next two sections we carry out this task, along the guidelines given in [15] and [11], leaving technical details to the Appendixes A and B.

III. RAINFALL FORCING

In dryland ecosystems, the temporal distribution of annual rainfall amounts may characteristically be partitioned into a wet and a dry season within each year, in the sense described in the Introduction. In light of such strong seasonal inhomogeneities in the occurrence and the intensity of rainfall, the parameters involved in any stochastic model proposed for the temporal rainfall process $P(t)$, spanning a sequence of several months, seasons, or years, ought to be considered fixed only over periods of scale considerably shorter than the annual or the seasonal scales, e.g., monthly or even weekly scales. Yet these parameters ought to be variable from each such period (e.g., month or week) to the next, within a given season or year, but ought to remain fixed for any such period across different years (at least under stable climatic conditions). Hereafter, we adopt the monthly scale as being appropriate for modeling the rainfall process $P(t|i)$ as a *homogeneous one-dimensional diffusion* on the closed interval $[0,+\infty)$, with *drift* coefficient $B_{P,i}$ and *dispersion* coefficient $A^2_{P,i}$, for $1 \le i \le 12$ indexing the 12 months of any given calendar year. That is, for the ith month of the year, the rainfall process is modeled as a solution of the Itô stochastic differential equation (SDE)

$$dP(t|i) = B_{P,i}[P(t|i)]dt + A_{P,i}[P(t|i)]dW(t). \tag{4}$$

driven by a standard Wiener process $\{W(t)\}$. For an introduction to the stochastic theory of diffusion processes, see [14]. Also see [16–18] regarding nonhomogeneous diffusion.

From a physical point of view, the drift represents the conditional expected rate of change of rainfall rate, for infinitesimal time increments, whereas dispersion controls the corresponding conditional variance of the fluctuations of rainfall rate about the drift, conditionally on a positive current state of rainfall rate. The shape of $B_{P,i}$ and $A^2_{P,i}$ depends on physical considerations about the growth and decay of rainfall intensity, but also on certain mathematical constraints required for the existence of proper solutions to Eq. (4).

Provided that a (strictly) stationary solution of Eq. (4) exists (i.e., positively recurrent or ergodic diffusion) for each i, then conditionally on raining (i.e., given that $P(t|i) > 0$), the probability density function (PDF)

$$f_{P,i,st}(p) = \frac{\mathcal{N}_{P,i}}{A^2_{P,i}(p)} \exp\left(\int^p \frac{2B_{P,i}(x)}{A^2_{P,i}(x)} dx \right) \tag{5}$$

of the invariant probability measure corresponding to the ith month is obtained from the well-known Fokker-Planck or Kolmogorov forward equation. $\mathcal{N}_{P,i}$ is a normalizing constant such that $\int_0^{+\infty} f_{P,i,st}(p)dp = 1$, while the argument of the exponential denotes the antiderivative function of $2B_{P,i}(x)/A^2_{P,i}(x)$, evaluated at $x=p$. Hereafter, we shall refer to $f_{P,i,st}$ as the stationary PDF of precipitation in the ith month of the year, conditionally on raining.

To address the invariant probability distribution of precipitation unconditionally, in a given month indexed by i, one must further specify the behavior of the corresponding diffusion model at the boundary points of its state space $[0,+\infty)$. According to [15], the right boundary $+\infty$ is considered *inaccessible* and the left boundary $\{0\}$ is necessarily *regular accessible*, since rain does stop eventually, rendering the unconditional invariant probability distribution of $P(t|i)$ *mixed*. This mixed distribution is comprised of an absolutely continuous component with PDF $f_{P,i,st}$ supported on the open interval $(0,+\infty)$ [i.e., conditionally on raining: $P(t|i) > 0$], and of a discrete component with a single atom probability $\mathbb{P}(P(t|i)=0) = (1+\psi_i/\mathcal{N}_{P,i})^{-1}$ supported at the boundary state $\{0\}$ [i.e., the event of not raining: $P(t|i)=0$]. Therefore, the cumulative distribution function (CDF) of the (unconditional) invariant probability measure of $P(t|i)$ is

$$F_{P,i,st}(p) = \frac{1}{1+\psi_i/\mathcal{N}_{P,i}} \left(1 + \frac{\psi_i}{\mathcal{N}_{P,i}} \int_0^p f_{P,i,st}(x)dx \right), \tag{6}$$

supported on all $p \ge 0$. The parameter ψ_i is a positive constant, ruling the transitions from the boundary $\{0\}$ (no rain) to the (raining) interior $(0,+\infty)$ of the state space $[0,+\infty)$, and vice versa, according to a nontrivial *sticky* boundary condition imposed at this boundary $\{0\}$; see [15]. Appendix A furnishes an explicit parametric family, Eqs. (A2) for modeling the stationary PDF of precipitation, obtained according to Eq. (5), for a specific pair of drift and dispersion coefficients, Eqs. (A1), postulated originally by [15,19]. A subfamily of those PDFs is adopted as a working model, fitted to observed precipitation data for each month of the year in Sec. V.

IV. COUPLED STOCHASTIC DYNAMICS OF S AND N AND THEIR STEADY-STATE PROBABILITY DISTRIBUTIONS

If the precipitation parameter P is upgraded so as to be considered a stochastic process $\{P(t)\}$, then the dynamical system described by Eqs. (1) becomes a system of SDEs, describing dynamics of the coevolving stochastic processes of degree of saturation $\{S(t)\}$ and of normalized vegetation density $\{N(t)\}$. In particular, if precipitation during the ith month of the year is modeled by a diffusion process $\{P(t|i)\}$, as suggested in Sec. III, then the smooth transformations $S(t|i) = S(P(t|i))$ and $N(t|i) = N(P(t|i))$ of $\{P(t|i)\}$, furnished by the steady-state solutions Eqs. (2) and (3), render both $\{S(t|i)\}$ and $\{N(t|i)\}$ as diffusion processes. That is, the transformed processes $\{S(t|i)\}$ and $\{N(t|i)\}$ solve the Itô SDEs, respectively,

$$\begin{aligned} dS(t|i) &= B_{S,i}[S(t|i)]dt + A_{S,i}[S(t|i)]dW(t), \\ dN(t|i) &= B_{N,i}[N(t|i)]dt + A_{N,i}[N(t|i)]dW(t), \end{aligned} \tag{7}$$

which are meant to be driven by the same Wiener process $\{W(t)\}$ driving Eq. (4) throughout time.

According to Itô's transformation formulas [see Eq. (B3) in Appendix B], the drifts $(B_{S,i}, B_{N,i})$ and dispersion coefficients $(A^2_{S,i}, A^2_{N,i})$ in Eqs. (7) are determined by those of precipitation $(B_{P,i}, A^2_{P,i})$ and the first two derivatives of the (smooth) transformations $S(P)$ and $N(P)$ expressed by Eqs. (2) and (3). Due to changes in the parameters of the drift and dispersion coefficients of P, from one month to another according to Eqs. (A1) in Appendix A, the drift and dispersion coefficients of S and N do vary as well. Ultimately, that

monthly variation of precipitation parameters propagates to the shape of the stationary probability distributions of S and N, while the system resides in either of its two steady states. Let $F_{S,i,st}$ and $F_{N,i,st}$ denote CDFs of invariant probability distributions corresponding to (strictly stationary) solutions $\{S(t|i)\}$ and $\{N(t|i)\}$ of Eqs. (7), for the ith month of the year.

In the bare soil steady state, $F_{S,i,st}$ is of mixed type. By analogy to the mixed CDF in Eq. (6), it is comprised of an absolutely continuous component with PDF $f_{S,i,st}$, supported on the open interval (0,1), and an atom probability supported at the left boundary $\{0\}$. The behavior of $\{S(t|i)\}$ at its regular accessible boundary $\{0\}$ is inherited directly from the "sticky" behavior of $\{P(t|i)\}$. Indeed, in the bare soil state, Eqs. (2), it is possible that $S(t|i)=s$, for every $s \in [0,1)$, but $S(t|i)=0$ if and only if $P(t|i)=0$, whence $\mathbb{P}(S(t|i)=0)=\mathbb{P}(P(t|i)=0)=(1+\psi_i/\mathcal{N}_{P,i})^{-1}$. On the other hand, $F_{N,i,st}$ is just a step function with a unitary jump discontinuity at $\{0\}$, due to total absence of vegetation. Therefore,

$$F_{S,i,st}(s) = \frac{1}{1+\psi_i/\mathcal{N}_{P,i}}\left(1+\frac{\psi_i}{\mathcal{N}_{P,i}}\int_0^s f_{S,i,st}(x)dx\right), \quad 0 \le s < 1,$$

$$F_{N,i,st}(n) = I_{[0,+\infty)}(n), \quad 0 \le n < 1. \tag{8}$$

In the vegetated steady state, both $F_{S,i,st}$ and $F_{N,i,st}$ are absolutely continuous functions, with corresponding PDFs $f_{S,i,st}$ and $f_{N,i,st}$, supported (respectively) by $s \in (\mu/\gamma, 1)$ and $n \in (0, 1-\mu/\gamma)$. That is, $F_{S,i,st}$ and $F_{N,i,st}$ are simply integrals of the corresponding PDF, since the boundaries μ/γ and 1 are inaccessible by the S process, and the boundaries 0 and $1-\mu/\gamma$ are inaccessible by the N process. The boundary constraints are consequences of the fact that all vegetated physical states require precipitation $P \in (\frac{\epsilon\mu w_1}{\gamma-\mu}, +\infty)$; see Sec. II. Therefore,

$$F_{S,i,st}(s) = \int_{\mu/\gamma}^s f_{S,i,st}(x)dx, \quad \frac{\mu}{\gamma} < s < 1,$$

$$F_{N,i,st}(n) = \int_0^n f_{N,i,st}(x)dx, \quad 0 < n < 1-\frac{\mu}{\gamma}. \tag{9}$$

Using Itô's formulas, a small effort of calculus demonstrated in Appendix B yields the PDFs $f_{S,i,st}$ and $f_{N,i,st}$ expressed analytically in terms of the precipitation PDF $f_{P,i,st}$ for both bare soil and vegetated states. The resulting expression for the bare soil state is

$$f_{S,i,st}(s) = \frac{\mathcal{N}_{S,i}}{\mathcal{N}_{P,i}} \frac{f_{P,i,st}\left(\frac{\epsilon w_1 s}{1-s}\right)}{(1-s)^2}, \quad 0 < s < 1, \tag{10}$$

and for the vegetated state the resulting expressions are

$$f_{S,i,st}(s) = \frac{\mathcal{N}_{S,i}}{\mathcal{N}_{P,i}} \frac{f_{P,i,st}\left(\frac{w_1[(\epsilon-\tau)\mu+\tau\gamma s]}{\gamma(1-s)}\right)}{(1-s)^2}, \quad \frac{\mu}{\gamma} < s < 1,$$

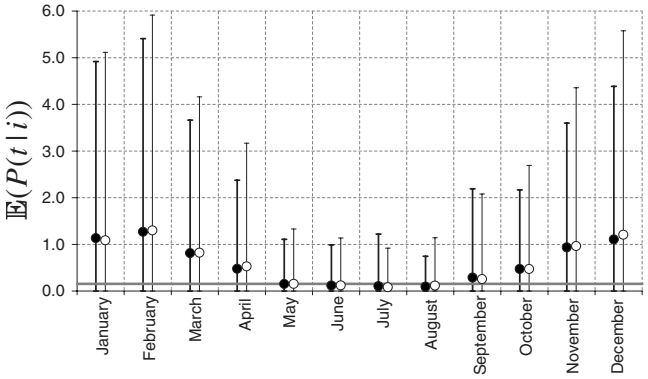

FIG. 1. Comparison between observed (●) and calculated (○) monthly means of daily rainfall with the relative standard deviation (error bars) at Skukuza, South Africa. The gray line represents the threshold value $P=\epsilon\mu w_1/(\gamma-\mu)$. All values are in m/yr.

$$f_{N,i,st}(n) = \frac{\mathcal{N}_{N,i}}{\mathcal{N}_{P,i}} \frac{f_{P,i,st}\left(\frac{w_1\mu[\epsilon(1-n)+\tau n]}{\gamma(1-n)-\mu}\right)}{[\gamma(1-n)-\mu]^2},$$

$$0 < n < 1-\frac{\mu}{\gamma}, \tag{11}$$

where $\mathcal{N}_{S,i}$ and $\mathcal{N}_{N,i}$ are normalizing constants, such that $\int_0^{+\infty} f_{S,i,st}(p)dp = 1 = \int_0^{+\infty} f_{N,i,st}(p)dp$. It is worthy of remark that Eqs. (8)–(11) are valid irrespective of the drift and dispersion coefficients $B_{P,i}$ and $A_{P,i}^2$, upon which a diffusion model for the precipitation process is built, and therefore also irrespective of the specific shape or form of the PDF $f_{P,i,st}$ given by Eq. (5).

V. THE ROLE OF RAINFALL SEASONALITY

In this section we investigate the role of rainfall seasonality on the soil-water vegetation dynamics, particularly with respect to the steady states. We try to understand how the rainfall abundance in certain periods of the year and the rainfall scarcity in other periods force the ecosystem toward the vegetated steady state or the bare soil state. With this goal, we refer to a 45-year (from 1960 to 2004) historical record of daily rainfall data observed at the Skukuza site, in the southern region of Kruger National Park, South Africa. The region's climate is semiarid subtropical with an average annual rainfall of about 575 mm. The maximum annual rainfall is 1116 mm, recorded in 2003, while the minimum is 274 mm, observed in 2000. Observations show high variability from month to month in any given year. An impression of this fact is depicted in Fig. 1, showing the sample mean and standard deviation of the daily rainfall for each given month of the year, across all years in the historical record. These statistics indicate sinusoidal variability with a maximum of 3.46 mm/day (i.e., 1.26 m/yr) observed in February, and a minimum of 0.26 mm/day (i.e., 0.09 m/yr) occurring in August. Since almost all the annual amount of rainfall (more than 93%) occurs in the period from September to April, we refer to this period as the wet season, and to the remaining months from May to August as the dry season.

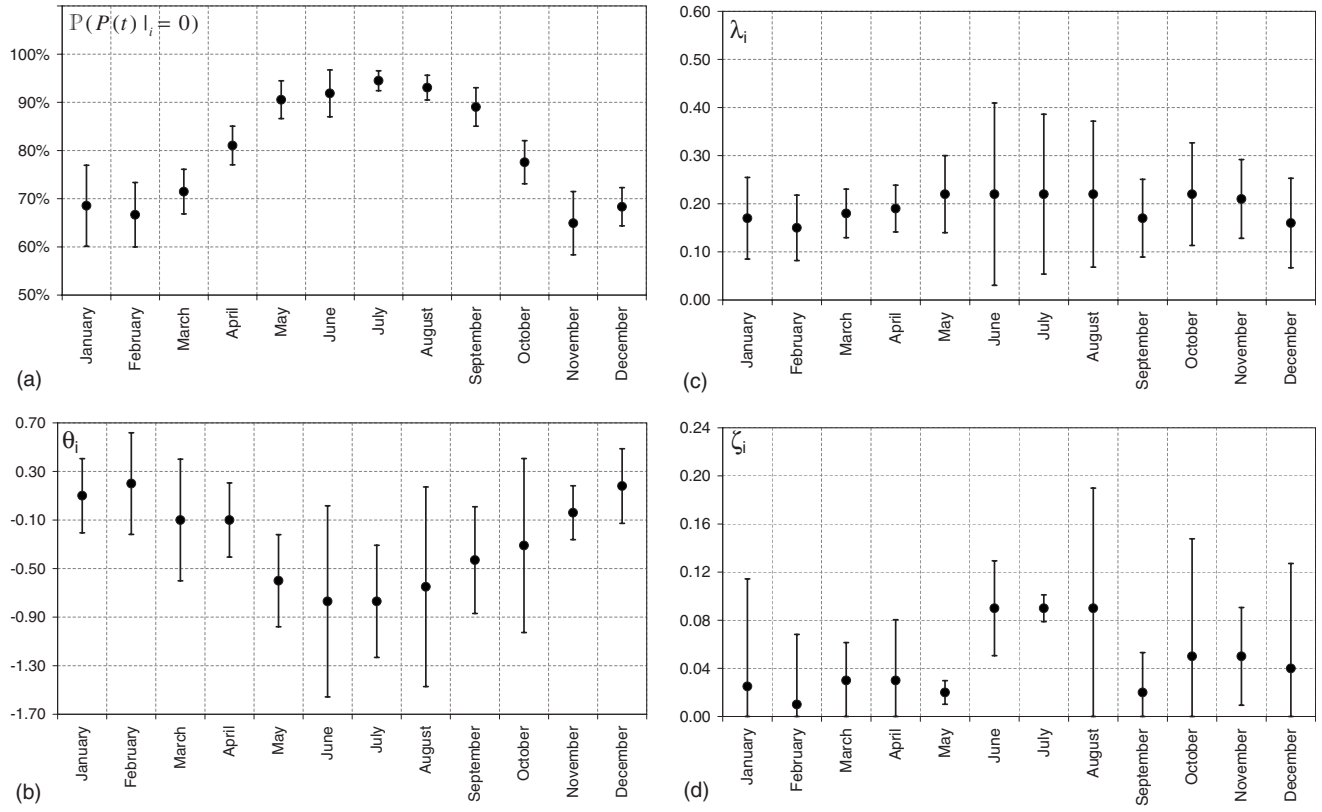

FIG. 2. Monthly estimates of the parameters of the P distribution, for Skukuza data set. Estimates of (a) $\mathbb{P}(P(t|i)=0)$, (b) θ_i, (c) λ_i, and (d) ζ_i. The standard deviation of estimate of each parameter is given as error bars.

Next, we consider the observed rainfall as a stochastic process, modeled during the ith month of any given year as a homogeneous diffusion $\{P(t|i)\}$ on $[0,+\infty)$, with drift and dispersion coefficients given by Eqs. (A1), with $\alpha_i=1$; see Appendix A. Consequently, the probability distribution model adopted to fit to rainfall data of each month is the mixed LST-lognormal distribution (defined in Appendix A), originally proposed in [15] and fitted to other precipitation data in [19]. The PDF of the absolutely continuous component of this mixed distribution is given by Eqs. (A2), for $\alpha_i=1$, involving three parameters, θ_i, λ_i, and ζ_i for each $1 \le i \le 12$. The atom probability $\mathbb{P}(P(t|i)=0)=(1+\psi_i/\mathcal{N}_{P,i})^{-1}$ of the event of no rainfall within the ith month is determined (under the model) by these three parameters $(\theta_i,\lambda_i,\zeta_i)$ through the normalizing constant $\mathcal{N}_{P,i}$ given by Eq. (A3), and by a fourth parameter $\psi_i>0$ representing the sticky boundary behavior suggested by [15].

In light of the historic data, θ_i, λ_i, and ζ_i have been estimated using the method of least squares. Subsequently, $\mathcal{N}_{P,i}$ is estimated by substituting the least square estimates of θ_i, λ_i, and ζ_i into Eq. (A3). The atom probability $\mathbb{P}(P(t|i)=0)$ is estimated by the sample percentage of zeros in the ith month of the year, across the historic record. Finally, substituting the estimates of $\mathcal{N}_{P,i}$ and $\mathbb{P}(P(t|i)=0)$ into the expression of $\mathbb{P}(P(t|i)=0)$, we obtain estimates of the sticky boundary parameters ψ_i. Figure 1 depicts also the unconditional mean value and the unconditional standard deviation of the invariant probability distribution of rainfall in each month of the year. These two characteristics are calculated through the formulas $\mathbb{E}(P(t|i))=\frac{\psi_i}{\psi_i+\mathcal{N}_{P,i}}\int_0^{+\infty} x f_{P,i,st}(x)dx$ and $[\mathrm{Var}(P(t|i))]^{1/2}=[\frac{\psi_i}{\psi_i+\mathcal{N}_{P,i}}\int_0^{+\infty} x^2 f_{P,i,st}(x)dx-\mathbb{E}(P(t|i))^2]^{1/2}$, for the (unconditional) mean and standard deviation, respectively (see [20]), using the estimated values of the parameters ψ_i and θ_i, λ_i, ζ_i in the analytical expressions Eq. (A3) for $\mathcal{N}_{P,i}$. The comparison between sample means and unconditional means of the fitted model, and between sample standard deviations and unconditional standard deviations of the fitted model, does indicate the adequacy of the adopted stochastic model for rainfall processes, in addition to the justifications already given in [11,15,19].

Sample estimates of $\mathbb{P}(P(t|i)=0)$ are shown in Fig. 2(a), along with least-squares estimates of the parameters θ_i, λ_i, and ζ_i, in Figs. 2(b)–2(d), respectively. Figure 2 gives also the standard deviation of estimates of each parameter, represented by error bars. The sample estimate and its standard deviation, for each parameter, are obtained from the nine nonoverlapping five-year segments comprising the 45-year rainfall record. The sample estimates of $\mathbb{P}(P(t|i)=0)$ exhibit a sinusoidal behavior with a maximum of 95% in July and a minimum of 65% in November. Notably, throughout the dry season the estimates of $\mathbb{P}(P(t|i)=0)$ remain greater than 90%. Sinusoidal variability is also indicated by the estimates of θ_i, while the other two parameters λ_i and ζ_i show a variability practically included within the error bars; thus λ_i and ζ_i could be assumed constant within the year, respectively equal to 0.19 and 0.05. Based on the estimated parameters θ_i, λ_i, and ζ_i, the LST-lognormal PDF $f_{P,i,st}$ of the invariant distribution of $\{P(t|i)\}$ for each month is computed and plot-

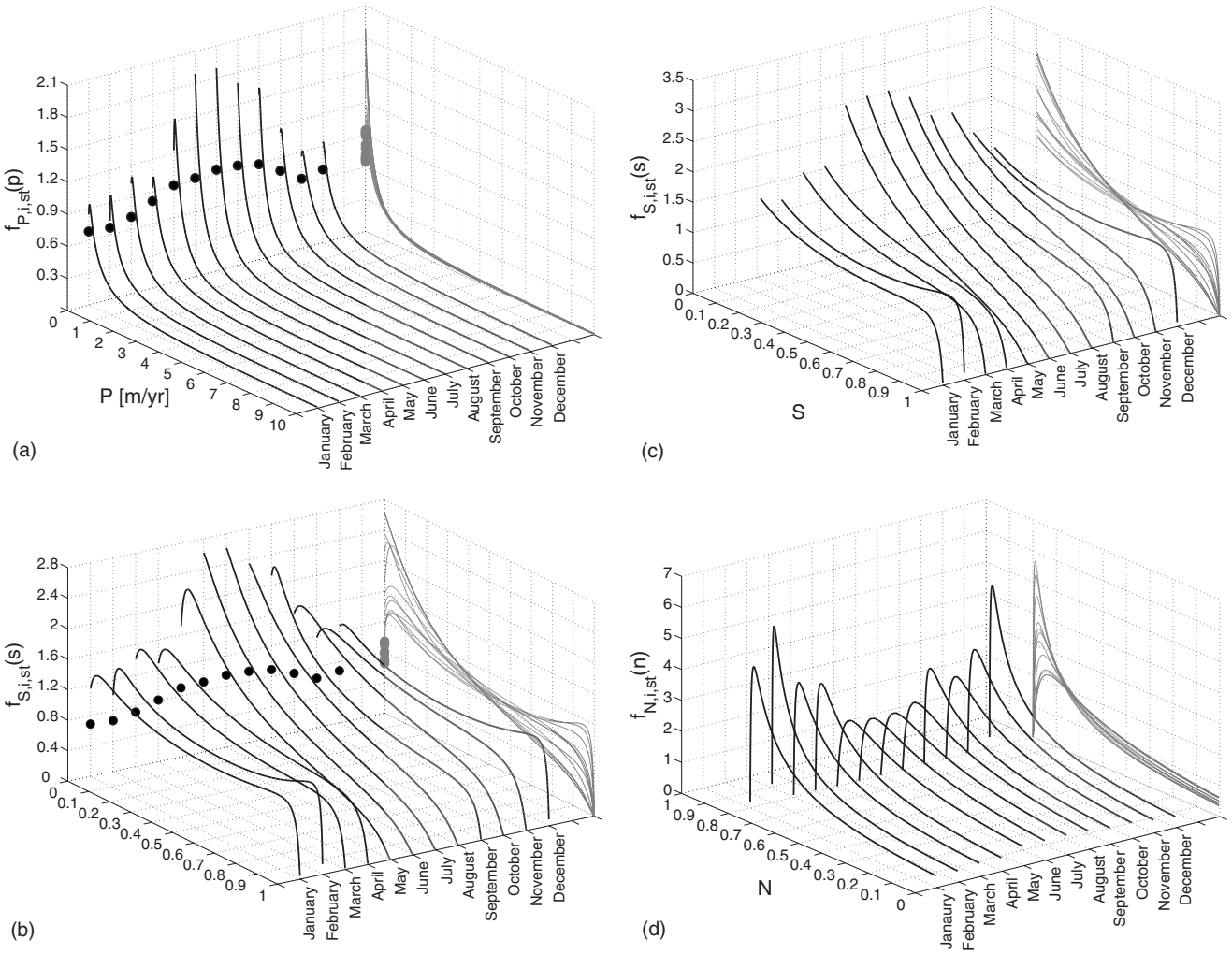

FIG. 3. Steady density function for the variables P, S, and N and for each month (black lines). (●) indicates the atom probability. (a) $f_{P,i,st}$, (b) $f_{S,i,st}$ for the bare soil case, (c) $f_{S,i,st}$, and (d) $f_{N,i,st}$ for the vegetated state. For a clear comparison among the 12 monthly densities, these are projected in the same plane (gray lines).

ted in Fig. 3(a), together with the corresponding sample estimates of atom probabilities $\mathbb{P}(P(t|i)=0)$. It is seen that in Fig. 3(a) the modal value (peak) of the PDF attains higher values during the dry season than during the wet season, confirming an intuitively anticipated effect, namely, that the likelihood of lower rainfall levels during the dry season dominates the likelihood of those levels in the wet season.

The parameters of Eqs. (1) are considered constant, and are assigned certain values as suggested in the literature, $w_1=0.35$ m, $\epsilon=4.0$ yr^{-1}, $\tau=5.0$ yr^{-1}, $\gamma=2.0$ yr^{-1}, and $\mu=0.4$ yr^{-1}; see [21]. These values are used throughout the rest of the present study. However, a sensitivity analysis with respect to these five parameters of Eqs. (1) has been recently shown in [11].

Figure 3(b) shows plots of $f_{S,i,st}$, the PDF of the invariant (mixed) probability distribution of $\{S(t|i)\}$ for each month, with respect to the bare soil steady state, including also the atom probabilities $\mathbb{P}(S(t|i)=0)=\mathbb{P}(P(t|i)=0)$ at the 0 boundary. Notably, $f_{S,i,st}$ is bimodal throughout the wet season, while during the dry season it becomes unimodal. This means that there are two preferential states (one close to $s=0$ and one close to $s=1$) for the soil water content during the period of rainfall abundance and only one (close to $s=0$) when rainfall is scarce. The bimodality of $f_{S,i,st}$ during the wet season is in agreement with data observation presented in [22,23].

Figure 3(c) shows plots of the PDF $f_{S,i,st}$, for each month, but with respect to the vegetated steady-state solution. Recall that in that case $f_{S,i,st}$ is supported only on the open interval $(\mu/\gamma,1)$, without any atoms of probability at either boundary. Similar considerations about the shapes of these PDFs are valid here as well as in the case of the bare soil solution. Figure 3(d) shows plots of the PDF $f_{N,i,st}$, for each month, of course in the vegetated steady-state solution. These PDFs $f_{N,i,st}$ are unimodal throughout the year. The mode is near the upper boundary, $n=1-\mu/\gamma$, causing negatively skewed probability distributions, more markedly so during the wet than in the dry season, to the effect that the likelihood of high levels of vegetation abundance is greater during the wet season than in the dry season. The negative skewness of $f_{N,i,st}$, especially during the dry season, signifies the resilience of vegetation to the water stress. Therefore, a first main conclusion to be drawn is that the seasonality of rainfall has a direct impact on the shape of probability distributions of

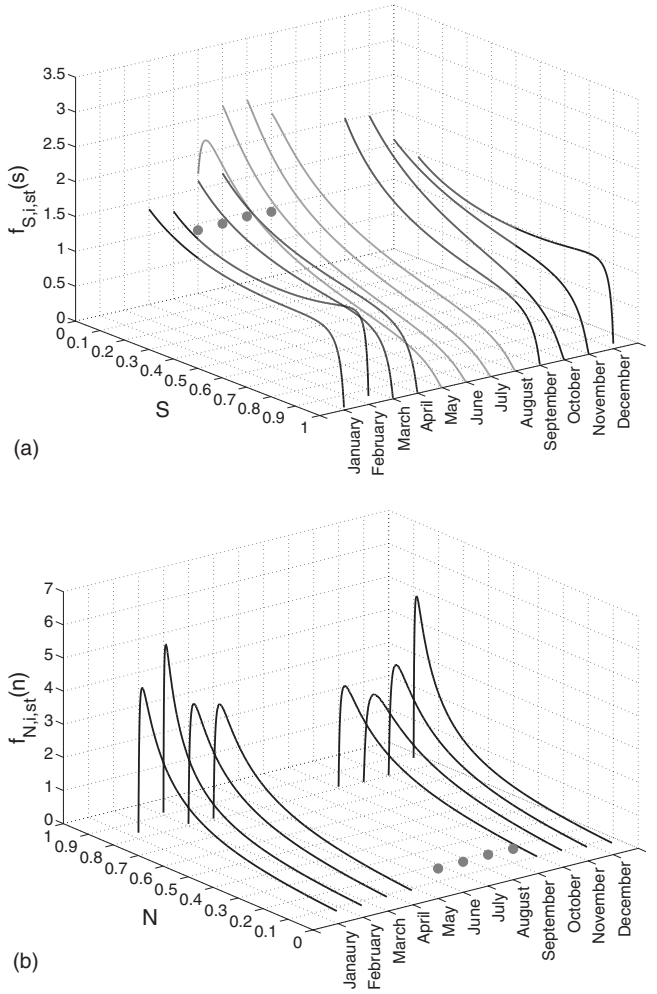

FIG. 4. Probability density function of the stable state solution for each month, for S in (a) and N in (b). The black line indicates that the stable solution is vegetated, and the gray line that the stable solution is unvegetated. (●) indicates the atom probability.

soil water and vegetation abundances associated with the two steady states of the ecosystem. For the adopted values of the parameters w_1, ϵ, τ, γ, and μ in Eqs. (1), the rainfall threshold $P=\frac{\epsilon\mu w_1}{\gamma-\mu}$ is approximately 0.15 m/yr (or 0.4 mm/day). Thus, for $P<0.15$ m/yr, only the bare soil steady state is attainable, which is locally stable, while for $P>0.15$ m/yr, both the vegetated and the bare soil steady states are attainable, of which only the vegetated one is locally stable. Figure 1 facilitates the comparison between the rainfall threshold level of 0.15 m/yr with the estimated mean of the daily rainfall for each month of the year across the historic record of data. In the period from September to April, the monthly mean of daily rainfall is greater than 0.15 m/yr, while in the period from May to August the monthly mean is lower than 0.15 m/yr. Thus, on average, during the dry season, the scarcity of rainfall forces the ecosystem soil-water vegetation toward the bare soil steady state, which is stable since rainfall remains below the critical threshold level. On the other hand, during the wet season, the abundance of rainfall pushes the system toward the vegetated steady state, which is also (locally) stable since rainfall remains above the critical threshold level. Figures 4(a) and 4(b) depict the PDFs of S and N, respectively, corresponding exclusively to the stable steady states, for each month. Thus, a second conclusion to be drawn is that the seasonality of rainfall causes the alternation between the two steady states of the system.

VI. CONCLUSIONS

In this paper we have studied the coupled dynamics of soil water and vegetation driven by a seasonally adjusted stochastic model of rainfall processes in drylands. The ecosystem oscillates between two steady states, one vegetated and one nonvegetated. The probability distributions of soil water and vegetation at those two steady states have been evaluated analytically. The impact of rainfall seasonality on the dynamics of the ecosystem has been addressed with respect to the (stable) steady states of the system. This seasonality causes changes in the shape of steady-state invariant probability distributions and forces an oscillation between the two steady states, namely, between the bare soil steady state, which remains stable during the dry season, and the vegetated steady state, which remains stable during the wet season.

ACKNOWLEDGMENTS

The financial support of the National Research Foundation of South Africa and Italian Ministry of Foreign Affairs is acknowledged. This work is a result of the bilateral project of scientific cooperation between Italy and South Africa titled "Rainfall, Fire, Elephant, and Tree Interactions in Southern African Savannas and Desertification." C.D.M. would like to thank Dr. Nadia Folcarelli and Dr. Redenta Maffettone of the Italian Ministry of Foreign Affairs.

APPENDIX A: A WORKING DIFFUSION MODEL FOR PRECIPITATION

The modeling of temporal processes of rain rate as homogeneous one-dimensional diffusions on the closed interval $[0,+\infty)$ was originally proposed in [15,19]. The drift and dispersion coefficients postulated therein, motivated by certain physical, mathematical, and empirical considerations, are nonlinear (logarithmic) mean reversion and power-law-type functions, respectively,

$$B_{P,i}=\lambda_i[\theta_i-\ln(P+\zeta_i)],$$

$$A_{P,i}^2=(P+\zeta_i)^{\alpha_i}. \tag{A1}$$

The index $1\le i\le 12$, introduced here, serves merely as the indication of the month, and the variation of the model's parameters, location $\theta_i\in\mathbb{R}$, scale $\lambda_i>0$, shape $\alpha_i>0$, shift $\zeta_i\ge 0$, from one month to another. The condition $\zeta_i>0$ is necessary and sufficient for the left boundary $\{0\}$ to be regular accessible, thereafter modeled by a further specification as a sticky boundary [15]. The PDF $f_{P,i,st}$ of the absolutely continuous component of the invariant probability distribution, obtained according to Eq. (5) for $p>0$, is

$$f_{P,i,st}(p) = \begin{cases} \dfrac{\mathcal{N}_{P,i}}{(p+\zeta_i)^{\alpha_i}} \exp\left[\dfrac{2\lambda_i (p+\zeta_i)^{1-\alpha_i}}{1-\alpha_i} \left(\theta_i + \dfrac{1}{1-\alpha_i} - \ln(p+\zeta_i) \right) \right], & \alpha_i \neq 1, \\ \dfrac{\mathcal{N}_{P,i}}{p+\zeta_i} \exp\{\lambda_i \theta_i^2 - \lambda_i [\ln(p+\zeta_i) - \theta_i]^2\}, & \alpha_i = 1. \end{cases} \tag{A2}$$

For $\alpha_i \neq 1$, the normalizing constant $\mathcal{N}_{P,i}$ must be computed numerically, since no closed expression is available. However, for $\alpha_i = 1$ one may analytically calculate

$$\mathcal{N}_{P,i} = 2 \frac{\exp(-\lambda_i \theta_i^2)}{\operatorname{erfc}(\xi_i)} \sqrt{\frac{\lambda_i}{\pi}}, \tag{A3}$$

where $\xi_i = (\ln \zeta_i - \theta_i)\sqrt{\lambda_i}$ and $\operatorname{erfc}(z) = 1 - \frac{2}{\sqrt{\pi}} \int_0^z \exp(-u^2) du$ is the complementary error function. In fact, the three-parameter subfamily of PDFs obtained from Eqs. (A2) when $\alpha_i = 1$ is referred to as the *left-shifted* (by ζ_i) and *left-truncated* (at 0) *lognormal* family, in short *LST-lognormal*. It is worth noting that the LST-lognormal family contains the two-parameter lognormal family of distributions, for $\alpha_i = 1$ and $\zeta_i = 0$, in which case $\theta_i = \mathbb{E}(\ln[P(t|i)])$ and $\lambda_i = 0.5/\mathrm{Var}(\ln[P(t|i)])$.

APPENDIX B: CALCULATION OF PDF BY ITÔ'S FORMULAS

Let $\{X(t)\}$ be a homogeneous one-dimensional diffusion process on an interval I, with drift coefficient B_X and dispersion coefficient A_X^2. Denote by s_X its *scale density function*

$$s_X(x) = \exp\left(- \int^x \frac{2B_X(\xi)}{A_X^2(\xi)} d\xi \right), \tag{B1}$$

and by m_X its *speed density function*

$$m_X(x) = \frac{1}{s_X(x) A_X^2(x)} = \frac{1}{A_X^2(x)} \exp\left(- \int^x \frac{2B_X(\xi)}{A_X^2(\xi)} d\xi \right). \tag{B2}$$

The PDF of the invariant probability distribution of the process, f_X, defined on the *interior* of the interval I, is a normalized version of the speed density. That is, $f_X(x) = m_X(x)\mathcal{N}_X$, where $\mathcal{N}_X$ is a constant, such that $\int_I f_X(x) dx = 1$; compare Eqs. (B2) and (5). If g is a real-valued function defined on I, possessing continuous derivatives up to second order in the interior of I, then Itô's transformation theorem renders the transformed stochastic process $\{Y(t) = g(X(t))\}$ a regular diffusion process in the interior of $g(I)$; e.g., see [14]. Itô's formulas specify the drift and dispersion coefficients of the transformed process $\{Y(t)\}$,

$$B_Y(y) = B_X(x) g'(x) + \frac{1}{2} A_X^2(x) g''(x),$$

$$A_Y^2(y) = A_X^2(x) [g'(x)]^2, \tag{B3}$$

at arguments x and y related by $y = g(x)$ or equivalently by $x = g^{-1}(y)$.

Substituting the expressions Eqs. (B3) into the integral defining the scale density function of $\{Y(t)\}$, and accounting for the change of variable $y = g(x)$, so that $dy = g'(x)dx$, one obtains

$$\begin{aligned} s_Y(y) &= \exp\left(- \int^{y=g(x)} \frac{2B_Y(\xi)}{A_Y^2(\xi)} d\xi \right) \\ &= \exp\left(- \int^x \frac{2\left[\frac{1}{2} A_X^2(\xi) g''(\xi) + B_X(\xi) g'(\xi) \right]}{A_X^2(\xi) [g'(\xi)]^2} g'(\xi) d\xi \right) \\ &= \exp\left[- \int^x \left(\frac{g''(\xi)}{g'(\xi)} + \frac{2B_X(\xi)}{A_X^2(\xi)} \right) d\xi \right] \\ &= \exp\left(- \int^x \frac{g''(\xi)}{g'(\xi)} d\xi \right) s_X(x), \end{aligned} \tag{B4}$$

furnishing the relationship between scale densities s_Y and s_X, for $y = g(x)$ or equivalently $x = g^{-1}(y)$. A similar calculation furnishes the following relationship between speed densities:

$$\begin{aligned} m_Y(y) = \frac{1}{s_Y(y) A_Y^2(y)} &= \frac{\exp\left(\int^x \frac{g''(\xi)}{g'(\xi)} d\xi \right)}{s_X(x) A_X^2(x) [g'(x)]^2} \\ &= \frac{\exp\left(\int^x \frac{g''(\xi)}{g'(\xi)} d\xi \right)}{[g'(x)]^2} m_X(x). \end{aligned} \tag{B5}$$

Ultimately, accounting for the normalizations $m_\cdot = f_\cdot / \mathcal{N}$, where $\cdot$ indicates either X or Y, between a speed density and the corresponding PDF, Eq. (B5), we obtain the following relationship between PDFs:

$$f_Y(y) = \frac{\mathcal{N}_Y}{\mathcal{N}_X} f_X(x) \frac{\exp\left(\int^x \frac{g''(\xi)}{g'(\xi)} d\xi \right)}{[g'(x)]^2}. \tag{B6}$$

When the role of g is played by the smooth transformations of precipitation in the steady-state solutions Eqs. (2) and (3), the corresponding PDFs in Eqs. (10) and (11) follow from Eq. (B6).

[1] M. Rietkerk, F. van den Bosch, and J. van de Koppel, Oikos **80**, 241 (1997).
[2] C. A. Klausmeier, Science **284**, 1826 (1999).
[3] J. von Hardenberg, E. Meron, M. Shachak, and Y. Zarmi, Phys. Rev. Lett. **87**, 198101 (2001).
[4] V. Guttal and C. Jayaprakash, J. Theor. Biol. **248**, 490 (2007).
[5] I. Rodriguez-Iturbe, A. Porporato, L. Ridolfi, V. Isham, and D. R. Cox, Proc. R. Soc. London, Ser. A **455**, 3789 (1999).
[6] I. Rodriguez-Iturbe and A. Porporato, *Ecohydrology of Water Controlled Ecosystems: Plants and Soil Moisture Dynamics* (Cambridge University Press, Cambridge, U.K., 2004).
[7] J. M. Nordbotten, I. Rodriguez-Iturbe, and M. A. Celia, Water Resour. Res. **43**, W01408 (2007).
[8] E. Istanbulluoglu and R. L. Bras, Water Resour. Res. **42**, W06418 (2006).
[9] W. Wang, B. T. Anderson, D. Entekhabi, D. Huang, R. K. Kaufmann, C. Potter, and R. B. Myeni, Earth Interact. **10**, 1 (2006).
[10] M. Baudena, G. Boni, L. Ferraris, J. von Hardenberg, and A. Provenzale, Adv. Water Resour. **30**, 1320 (2007).
[11] C. De Michele, R. Vezzoli, H. Pavlopoulos, and R. J. Scholes, Ecol. Modell. **212**, 397 (2008).
[12] P. F. Ffolliott, K. N. Brooks, H. M. Gregersen, and A. L. Lundgren, *Dryland Forestry: Planning and Management* (John Wiley & Sons, New York, 1995).
[13] P. K. Patra, M. Ishizawa, S. Maksyutov, T. Nakazawa, and G. Inoue, Global Biogeochem. Cycles **19**, GB3005 (2005).
[14] S. Karlin and H. M. Taylor, *A Second Course in Stochastic Processes* (Academic Press, New York, 1981).
[15] H. Pavlopoulos and B. Kedem, Commun. Stat. Stoch. Models **8**, 397 (1992).
[16] V. Giorno, A. G. Nobile, and L. M. Ricciardi, Adv. Appl. Probab. **19**, 974 (1987).
[17] R. Gutiérrez, L. M. Ricciardi, P. Román, and F. Torres, J. Appl. Probab. **34**, 623 (1997).
[18] V. Wirth, Phys. Rev. E **64**, 016136 (2001).
[19] B. Kedem, H. Pavlopoulos, X. Guan, and D. A. Short, J. Appl. Meteorol. **33**, 1486 (1994).
[20] A. M. Mood, F. A. Graybill, and D. C. Boes, *Introduction to the Theory of Statistics* (McGraw-Hill, Singapore, 1986).
[21] R. J. Scholes and B. H. Walker, *An African Savanna: Synthesis of the Nylsvley Study* (Cambridge University Press, Cambridge, U.K., 1993).
[22] P. D'Odorico and A. Porporato, Proc. Natl. Acad. Sci. U.S.A. **101**, 8848 (2004).
[23] A. J. Teuling, R. Uijlenhoet, and P. Troch, Geophys. Res. Lett. **32**, L13402 (2005).